Florida State University

Innovative Proton Conducting Membranes for Fuel Cell Applications & Protein Enhanced Proton Conduction Membranes for Advanced Fuel Cells

PI: Ongi Englander, Anant Paravastu **Co-PIs:** Anter Al-Azab, Subramanian Ramakrishnian
Students: Erin Holley, MS Materials Science and Nicola Kissoon, MS Materials Science

Description: To meet Florida's sustainable energy demands, we will develop membranes capable of supporting high efficiency proton conducting nanomaterials. Novel membranes will include materials based on colloidal assembly of surface-modified silica particles and the fabrication of silica and latex-supported membranes

Budget: $30,000
Universities: FSU

Progress Summary

The work performed here was the basis of Master's thesis of Erin Holley who graduated in August 2010. The highlights of this work are described below.

1) *Synthesis and Characterization of Latex Composite Membranes: Monodisperse Particles*
Particles of 200 nm, 650 nm and 900 nm were successfully synthesized using an emulsion polymerization technique. Membranes were then fabricated by depositing these particles on commercial supports and by heat stabilizing them.

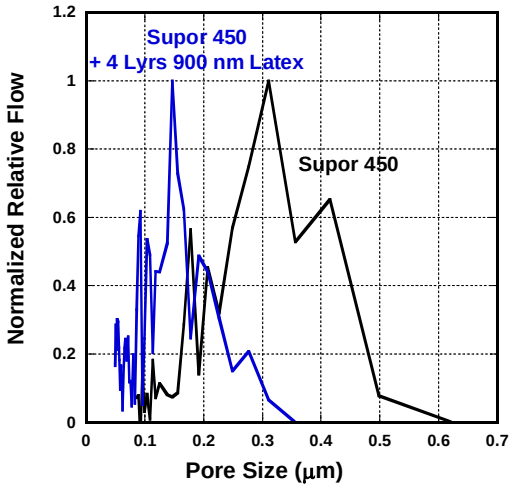

Figure 1: Pore size distribution of Supor 450 and 4 layers of 900nm latex deposited on top of Supor 450.The peak in pore size decreases to lower pore sizes with addition of particles and also results in a narrower pore size distribution.

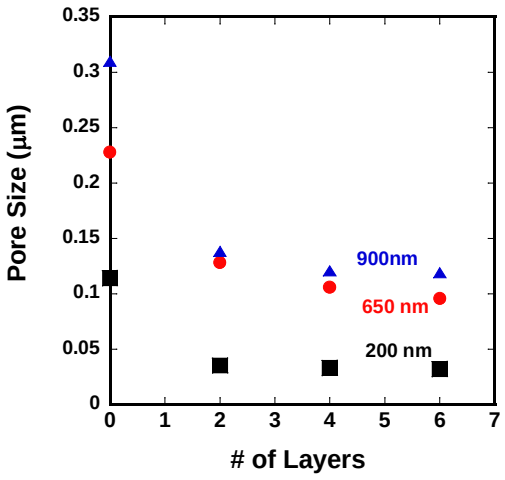

Figure 2: Pore size as a function of number of layers for different size particles used in this work.

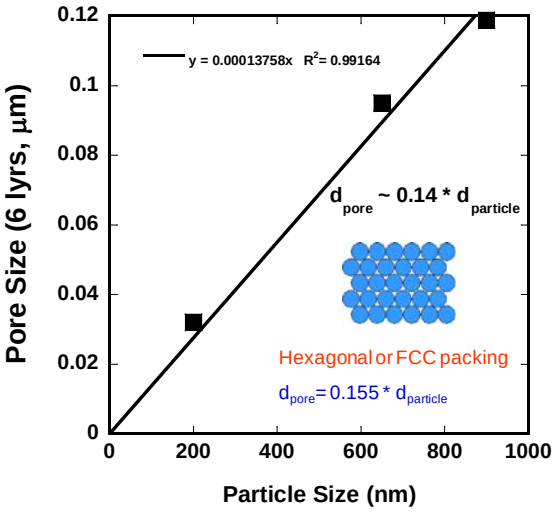

Figure 3. Pore size for 6 layers of particles as a function of particle size. It is found that the pore diameter is approximately 14 % of the particle size which is slightly lower than a hexagonal or FCC packing.

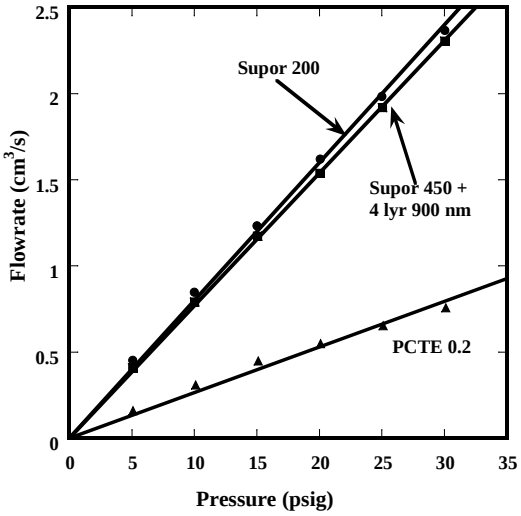

Figure 4: Comparison of water flow rate data for Supor 200, Supor 450 with approximately 4 layers of deposited 900 nm polystyrene particles, and PCTE 0.2.

Table 1. Gas characterization data for single size latex composite membranes.

Composite Membrane Description	Approximate Number of Layers N	Weight of Deposited Latex W (g/cm²)	Mean Pore Size d (µm)
Supor 100 + 200 nm	2	2.984×10^{-5}	0.0351
	4	5.968×10^{-5}	0.0340
	6	8.952×10^{-5}	0.0330
Supor 200+ 650 nm	2	9.746×10^{-5}	0.1279
	4	1.949×10^{-4}	0.1204
	6	2.924×10^{-4}	0.0958
Supor 450 + 900 nm	2	1.323×10^{-4}	0.1383
	4	2.646×10^{-4}	0.1205
	6	3.969×10^{-4}	0.1207

Figure 4 demonstrates that when 4 layers of 900 nm particles are deposited on a base membrane of Supor 450, a water flux comparable to that of Supor 200 is achieved. The advantage here is that the latex composite membrane has a pore size of 0.12 microns while the Supor 200 has a pore size of 0.23 microns. Thus using this technology one has formed a membrane with a narrower pore size and higher flux.

2) *Synthesis and Characterization of Latex Composite Membranes: Particle Mixtures*

The aim here is to mixtures of particles to narrow the pore size distribution. The hypothesis is that the smaller particles will pack in the voids of the bigger particles and result in a smaller pore size.

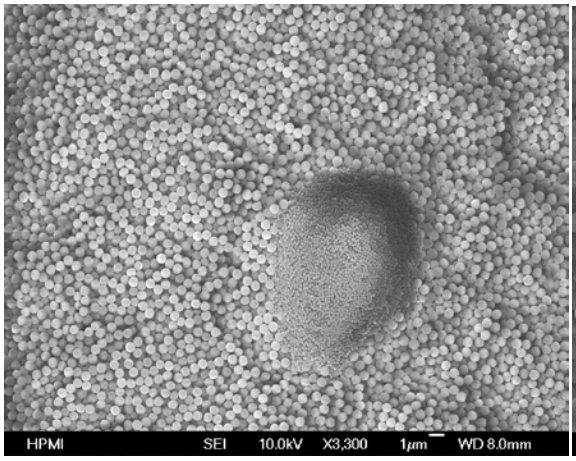

Figure 5: SEM (top view) of a layered structure. 2 layers 650nm/ 2 layers 200nm on commercial Supor 200.

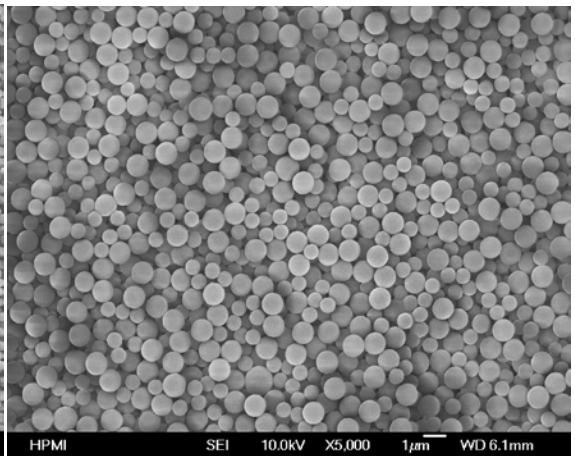

Figure 6: SEM (top view) of the membrane: 2 layers 900nm + 2 layers 650 nm Mixture on Supor 450

Figure 5 above is an SEM of a membrane in which 200nm particles were deposited on 650 nm particles and the membrane dried in an oven. This is resulted in the 200 nm particles clumping together – either due to the drying process or due to phase separation. This problem was overcome by mixing the two particles before deposition and by filtering the mixture onto the substrate. Figure 6 is a picture of the resultant membrane. As can be seen from this figure, the problem of the smaller particles clumping together is overcome by this technique. The pore sizes of the resultant membranes are given in Table 2.

Table 2: Synthesized membranes and their pore sizes.

Membrane Description	Average Pore Size (microns)
2 layers 650 nm on Supor 200	0.13
2 layers 200 nm on Supor 100	0.035
2 layers 650nm/ 2 layers 200 nm on Supor 200	0.086
Mixture 2 layers 650nm + 2 layers 200 nm on Supor 200	0.032

As can be seen from Table 2, it is possible to take a macroporous support such as Supor 200 which has a pore size of 0.22 microns (220 nm) and to narrow and reduce the pore size to 0.032 microns or 32 nm. If the particles clumped together as seen in Figure 4, then a higher pore size of 86 nm was achieved.

Table 3: Water flux and resistance values for dual size mixed polystyrene latex composite membranes.

Membrane Description	Approximate Number of Layers for Second Particle Size, N	Weight of Deposited Latex W (g/cm²)	Resistance of Composite Membrane R_M x 10^{-8} (cm^{-1})	Water Flux Composite Membrane J (cm/min) 10 psi
Supor 200 + 2 Layers 650 nm + N Layers 200 nm	2	2.984 x 10^{-5}	926	0.0487
	4	5.968 x 10^{-5}	1059	0.0455
	6	8.952 x 10^{-5}	7941	0.0790
Supor 450 + 2 Layers (1.323 x 10^{-4} g/cm²) 900 nm + N Layers 650 nm	2	9.746 x 10^{-5}	6.38	6.86
	4	1.949 x 10^{-4}	9.51	4.62
	6	2.924 x 10^{-4}	10.98	4.68

Table 4: Mean pore sizes for layered and mixed bidispersed polystyrene composite membranes.

Composite Membrane Description	Packed Bed Description	Mean Pore Size d (μm)
Supor 200 + 2 Layers 650 nm + 2 Layers 200 nm	Layered	0.0859
	Mixture	0.0324
Supor 200 + 2 Layers 650 nm + 4 Layers 200 nm	Layered	0.0795
	Mixture	0.0315
Supor 200 + 2 Layers 650 nm + 6 Layers 200 nm	Layered	0.0900
	Mixture	0.0319
Supor 450 + 2 Layers 900 nm + 2 Layers 650 nm	Layered	0.1411
	Mixture	0.0890
Supor 450 + 2 Layers 900 nm + 4 Layers 650 nm	Layered	0.1424
	Mixture	0.0831
Supor 450 + 2 Layers 900 nm + 6 Layers 650 nm	Layered	0.1324
	Mixture	0.1024

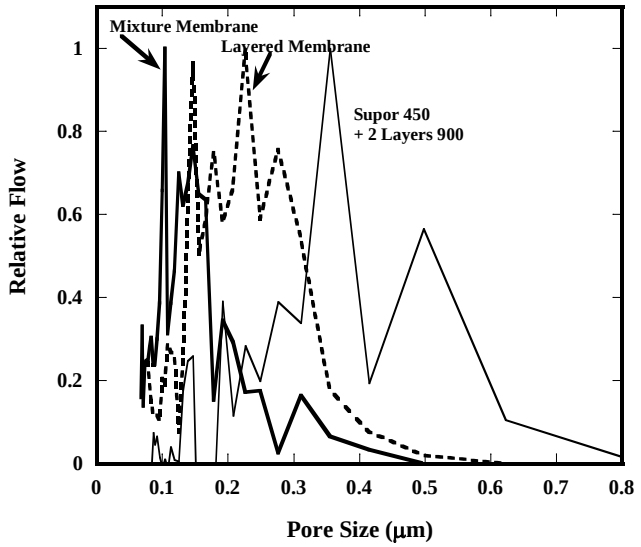

Figure7: Relative flow (normalized) as a function of pore size for layered and mixture membranes involving approximately 2 layers of 900 nm particles and approximately 2 layers of 650 nm particles on Supor 450. As can be seen the misture membrane had a lower pore size and a narrower pore size distribution.

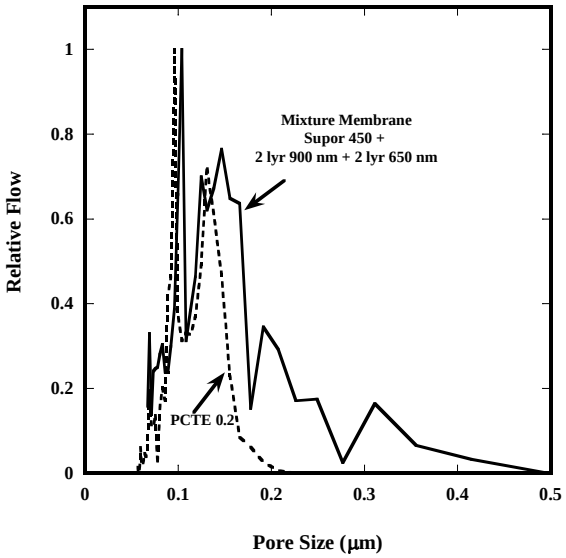

Figure 8: Comparison of normalized relative flow as a function of pore size for PCTE 0.2 and mixture membrane made up of 2 layers 900 nm and 2 layers of 650 nm particles on Supor 450.

Figure 8 clearly demonstrates that it is possible to take a porous substrate and modify the pore size distribution using latex particles and to yield smaller pore sizes. Figure 9 below is a comparison of the water flow rate for the mixture membrane and commercial PCTE 0.2. Figure 8 and 9 prove that it is possible to create composite membranes with narrow pore size distributions and low resistances to water

flux. The mixture membrane shown allows for higher water flux than the commercial PCTE 0.2 membrane.

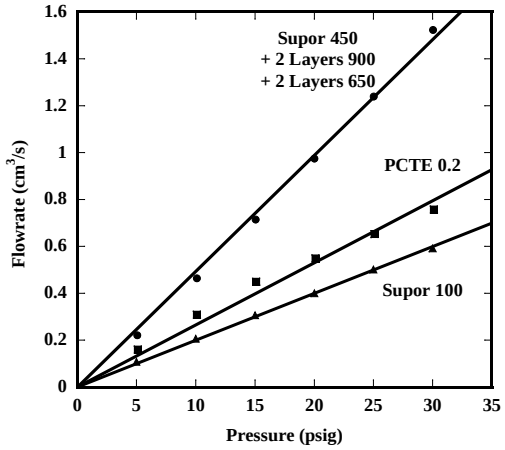

Figure 9: Comparison of flow rate as a function of applied pressure for Supor 100, PCTE 0.2, and mixture membrane made up of 2 layers 900 nm and 2 layers of 650 nm particles on Supor 450.

Task 2: Incorporation of protein nanomaterials inside silica membranes

Physical incorporation of protein nanofibers into silica-based membranes will require preparation of highly pure well dispersed protein nanofiber systems. Additionally, the functional integration of these materials with silica membranes requires that their electrical transport properties become better understood. Thus, our efforts have focused on the synthesis of well-dispersed protein nanofibers and their integration with microfabricated electrodes as a means for the evaluation of electrical transport properties. This work will be presented at the ASME IMECE2010 conference this November.

Progress to Date

The work performed here is the basis of Master's thesis of Nicola Kissoon who will graduate in Fall 2010 or Spring 2011. The highlights of this work are described below.

Synthesis of well-dispersed nanofiber arrays

We seek to define the parameters which yield dense yet well-dispersed nanofiber arrays and avoid higher order aggregation and the formation of sheet-like structures. Thus, we focused our assessment on the role of initial solution concentration, and the number and time between self-seeding events on the resulting nanofiber network. The differences in concentration and self-seeding intervals provide insight to their effect on self-assembly and aggregation. We find that the particular sample preparation procedures significantly affect the resulting nanofiber arrays. We have carried out a systematic study to evaluate the role of concentration, number of self-seedings and time between self-seeding on resulting sample dispersity. We have observed benefits of *self-seeding* where freshly seeded nanofiber matrices (small aliquots of nanofiber solutions) are sonicated and added back to increase conversion of monomers. We suspect that self-seeding helps reduce the negative impact of fiber-fiber interactions on seed effectiveness.

We present a few of the results in Figure 10 below. At this time, we can conclude that lower concentrations may be better suited for providing well-dispersed samples. These experiments suggest that there is an optimal number of self-seeding events as samples following one self-seeding event and many self-seeding events do not exhibit the desirable characteristics that are noted following few self-seeding events. Although very preliminary, it appears that following 2 self-seeding events (3 days/3 hours), the best sample dispersity is obtained. These results also suggest that number of self-seedings rather than time is more critical to achieving well-dispersed samples. We note aggregation at both early and late time potentially due to different mechanisms such as fiber fragments and/or unreacted domains. We also note that these results are unique to Aβ and specifically its growth and self-assembly kinetics. Since our initial studies yielded fairly dense results, the initial concentration of Aβ peptide was reduced in an attempt to

better control the density of the resulting nanofiber networks. A dense yet well-dispersed nanofiber network integrated with the electrodes is achieved following two self-seeding events performed at 24 hour intervals. Further, to assess the role of the time between self-seedings, we explore a significantly shorter time interval. A one-hour interval between both the initial and subsequent self-seeding events is selected. The results are favorable in terms of controlling densities although larger scale aggregates are present.

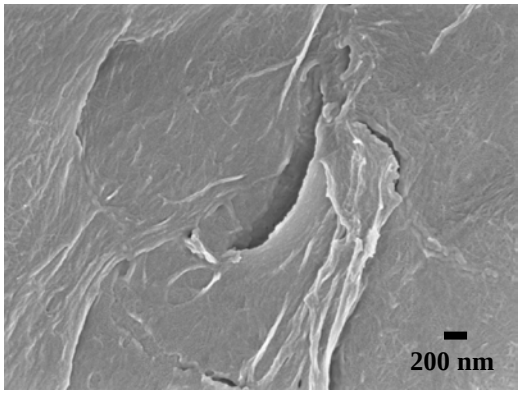

(a) An SEM image of a 0.05 mg/mL (67% seeding) Aβ solution made at two hours (one 5% self-seeding by volume).

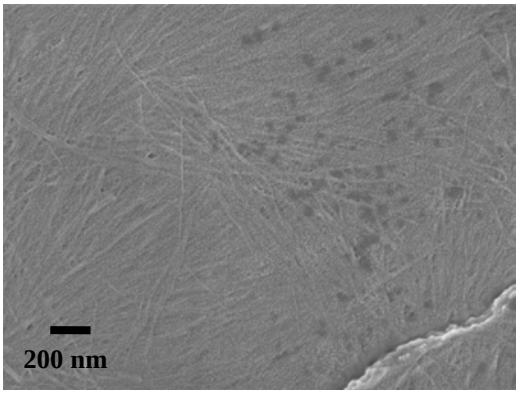

(b) *An SEM image of a 0.05 mg/mL (67% seeding) Aβ solution prepared at three hours (two 5% self-seedings by volume).

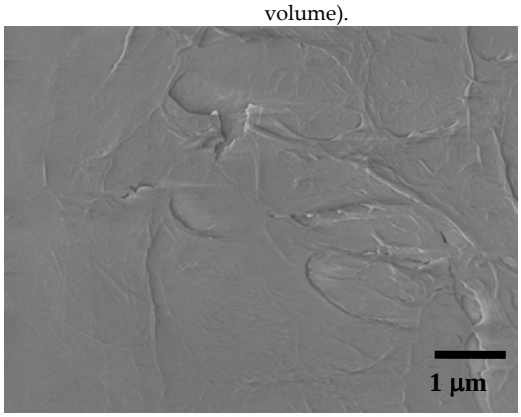

(c) An SEM image of a 0.05 mg/mL (67% seeding) Aβ solution and prepared at two hours (one 10% self-seeding by volume).

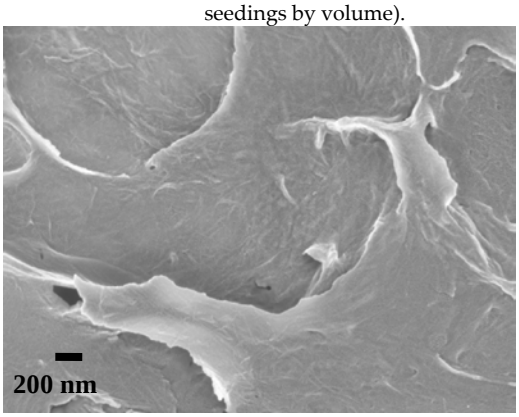

(d) An SEM image of a 0.05 mg/mL (67% seeding) Aβ solution and prepared at three hours (two 10% self-seedings by volume).

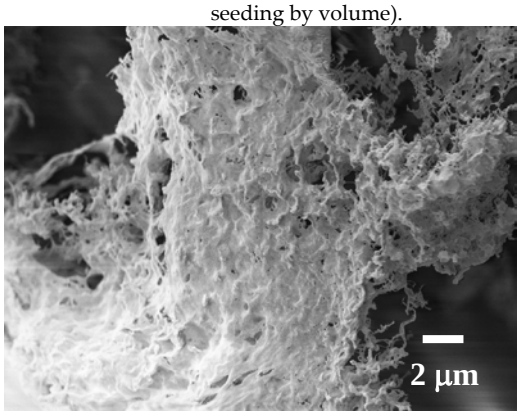

(e) An SEM image of a 1mg/mL, (9% seeding) Aβ solution 4-6 hours following seeding (no self-seeding).

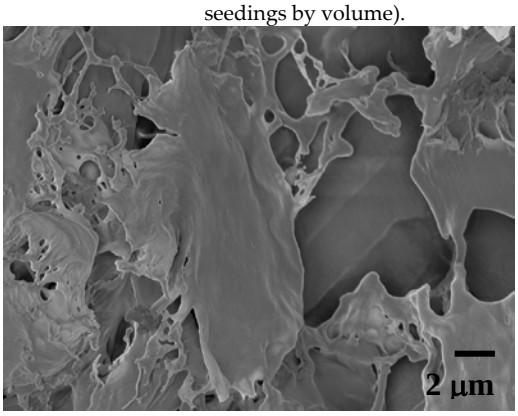

(f) An SEM image of a 0.6 mg/mL (14% seeding) Aβ solution prepared two days following initial preparation (one 10% self-seeding by volume).